Non-linear conductance of disordered quantum wires

2000 J. Phys.: Condens. Matter 12 8995

(http://iopscience.iop.org/0953-8984/12/42/306)

J. Phys.: Condens. Matter **12** (2000) 8995–9006. Printed in the UK PII: S0953-8984(00)14707-1

Non-linear conductance of disordered quantum wires

T N Todorov

School of Mathematics and Physics, The Queen's University of Belfast, Belfast BT7 1NN, UK

E-mail: t.todorov@qub.ac.uk

Received 14 June 2000, in final form 27 July 2000

Abstract. The self-consistent electron potential in a current-carrying disordered quantum wire is spatially inhomogeneous due to the formation of resistivity dipoles across scattering centres. In this paper it is argued that these inhomogeneities in the potential result in a suppression of the differential conductance of such a wire at finite applied voltage. A semi-classical argument allows this suppression, quadratic in the voltage, to be related directly to the amount of intrinsic defect scattering in the wire. This result is then tested against numerical calculations.

1. Introduction

In recent years it has been possible experimentally to produce laterally confined conductors, often referred to as quantum wires, with a transverse size not much larger than the Fermi wavelength of the electrons. One example of such a conductor is a constriction in a two-dimensional electron gas in a semiconductor heterostructure [1, 2]. Another example is that of three-dimensional metallic nanojunctions, produced using mechanically controllable break junctions [3, 4] or scanning tunnelling and atomic force microscopes [5–7].

Modelling work has studied the relation between the zero-voltage conductance of nanowires and their underlying atomic structure and geometry. Atomistic simulations combined with conductance calculations [8–11] explained the experimentally observed jumps in the zero-voltage conductance [3–7] and in the applied tensile force [12–14] during wire pull-off in terms of abrupt atomic rearrangements in response to the applied strain. Conductance calculations on static geometries [15, 16] and further atomistic simulations [17, 18] investigated the effect of shape and internal structure on the experimentally observed quantization, in units of $G_0 = 2e^2/h$, of the zero-voltage conductance of nanoscale metallic constrictions [6, 7, 19–22].

Another electrical conduction property of quantum wires that can be measured in experiment is their differential conductance as a function of applied voltage. Theoretical models have related non-linearities in the differential conductance, as a function of voltage, of ballistic constrictions to their energy subband structure [23–28]. The purpose of the present paper is to relate the finite-voltage differential conductance of disordered quantum wires in the elastic, phase-coherent regime to the intrinsic disorder in them. One aspect of this problem is the relation between elastic scattering and conductance fluctuations [29]. Here we consider another aspect.

Below, it is argued that spatial inhomogeneities in the self-consistent electron potential in a current-carrying disordered wire result in an overall suppression of the differential conductance as a function of voltage. This suppression is directly related to the amount of intrinsic defect scattering in the wire, because the spatial inhomogeneities in the potential, causing the

0953-8984/00/428995+12$30.00

suppression, originate from the formation of resistivity dipoles across the scattering centres in the wire. A semi-classical argument, given in the next section, gives a model relation between the suppression of the conductance and the quantity L/l_0, where L is the length of the wire and l_0 is the mean free path of the electrons in it. This relation is tested against numerical calculations in section 3. Section 4 contains a discussion and a summary of the results in the paper.

2. Simple model

We consider the following set-up. We imagine a quantum wire of length L, with a uniform cross-section. The wire contains a random distribution of defects, giving rise to phase-coherent electron scattering with a mean free path l_0. Each end of the wire is connected to a macroscopic electrode. The two electrodes, which are identical, are biased relative to each other by the application of a battery of voltage W, producing a flow of electrons from left to right.

The variation of the self-consistent one-electron potential along such a system is known [30–34]. If the wire is perfect, then the potential deep inside each electrode and deep inside the wire is constant, and the potential drops occur through the contacts between the electrodes and the wire. If there is scattering in the wire, then the potential drop occurs partly through the contacts and partly through the wire. At finite bias, these potential variations along the system constitute an additional scattering mechanism for the conduction electrons. Let us consider its effect on the finite-voltage differential conductance of the wire.

The self-consistent electron scattering in a current-carrying disordered conductor results in a concentration of the electric field across scattering centres, through the formation of residual resistivity dipoles around obstacles to current flow [31, 33, 35–38] (see also [39] and further references therein). Our first assumption is that the wire is sufficiently wide, and the defects in it are sufficiently dilute, that a well-defined resistivity dipole forms around each defect. Let us think of the potential in our system in the following way [33]. We imagine a smooth average background potential profile, with a total drop equal to the battery voltage W, extending from deep inside the left electrode, through the wire, to deep inside the right electrode. This average background potential is symmetric about the mid-point of the wire, which should be true at least in the small-voltage limit. Superimposed on the background potential is a set of resistivity-dipole potentials, each centred at a defect in the wire and each consisting of a potential hump in front of the defect and a potential trough behind the defect.

Next, we ignore electron backscattering by the background potential. For a given applied voltage W, this will require the length of the system to be sufficiently large to ensure that the gradient of the background potential profile is everywhere sufficiently small to allow this background potential to be treated as an adiabatic semi-classical potential. All electron scattering in the wire at finite voltage, then, is due to the intrinsic defects and to the resistivity-dipole potentials around these defects.

We make two more approximations. We ignore electron backscattering at the contacts between the wire and the electrodes, and we assume that eW is much less than the energy subband spacing in the wire so that the number of open conduction channels, N, in the wire is constant over an energy window eW around the Fermi level. Then, using the Landauer conductance formula [40], for the electron current in the system $I = I(\mu, W)$ we write

$$I = \frac{2eN}{h} \int_{\mu - eW/2}^{\mu + eW/2} T(E, W)\, \mathrm{d}E \tag{1}$$

where μ is the position of the Fermi level in the absence of the applied voltage, and

$$NT(E, W) = \sum_{n=1}^{N} T_n(E, W)$$

with $T_n(E, W)$ being the probability that an electron entering channel n in the biased wire, from the left electrode, will be transmitted through the wire, to the right electrode.

Next, we invoke the semi-classical result [41]

$$\langle T(E, W)\rangle = 1/(1 + L/l) \tag{2}$$

where the angular brackets designate averaging over different defect configurations, and, to within a factor of order unity, l is the mean free path of electrons with energy E in the disordered biased wire. We assume that the intrinsic defects and the resistivity-dipole potentials within the wire can be treated as two independent scattering mechanisms, satisfying Matthiessen's additivity rule, and write

$$1/l = 1/l_0 + 1/l_W \tag{3}$$

where l_W is the electron mean free path for scattering by the dipole potentials. In general, l_0 and l_W will be functions of the electron energy E in equations (1) and (2).

Consider l_W. It is given by

$$1/l_W = n\sigma_W = (n\sigma_d)(\sigma_W/\sigma_d) = (1/l_0)(\sigma_W/\sigma_d) \tag{4}$$

where n is the density of the resistivity dipoles, which is the same as that of the intrinsic defects, σ_d is the scattering cross-section of a defect and σ_W is the scattering cross-section of its resistivity dipole. Like l_0 and l_W, σ_d and σ_W are functions of E.

Treating the dipoles as weak scatterers, we assume that σ_W is proportional to the square of the amplitude of a resistivity-dipole potential. This amplitude must in turn be proportional to the electron current density, incident on the defect. In the extreme limit where this defect is the only defect in the wire, this current density is the unperturbed current density that would flow in the defect-free wire. Hence, in that limit, to lowest order in W, we have $\sigma_W = \sigma_W^0 W^2$, where σ_W^0 is a constant that is independent of W but is, in general, a function of the electron energy E. In the opposite limit, where there are many defects in the wire and electron flow through it is diffusive, the current density incident on a defect is essentially the same as the average current density in the specimen. Hence, in this limit we write $\sigma_W = \sigma_W^0 W^2/(1 + L/l_0)^2$. As a trial form, for the intermediate regime we write

$$\sigma_W = \sigma_W^0 W^2/(1 + L/l_0)^\nu \tag{5}$$

where ν is an empirical exponent, with $0 \leqslant \nu \leqslant 2$.

Combining equations (1) to (5), for the configurationally averaged current in the system we obtain

$$\langle I\rangle = \frac{2eN}{h}\int_{\mu - eW/2}^{\mu + eW/2} \frac{1}{1 + x + xsW^2/(1 + x)^\nu}\,\mathrm{d}E \tag{6}$$

where $x = x(E) = L/l_0$ and $s = s(E) = \sigma_W^0/\sigma_d$.

Let now $G = G(\mu, W) = \partial I/\partial W$ be the differential conductance at bias W. After configurational averaging, from equation (6) to lowest order in W we obtain

$$\langle G\rangle = \langle g\rangle - 3G_0 NsW^2\, x/(1 + x)^{2+\nu} \tag{7}$$

where $s = s(\mu)$, $x = x(\mu)$ and

$$g = g(\mu, W) = [G(\mu + eW/2, 0) + G(\mu - eW/2, 0)]/2. \tag{8}$$

Equation (7) states that the configurationally averaged differential conductance $\langle G\rangle$, as a function of W, is suppressed below the reference quantity $\langle g\rangle$ by an amount, quadratic in W and proportional to $x/(1+x)^{2+\nu}$. The quantity $x = L/l_0$, in turn, is a measure of the amount of scattering in the wire and may be used to differentiate between the ballistic, diffusive and localization regimes in the wire [41]. Equation (7) therefore gives a direct relation between the finite-voltage differential conductance and the intrinsic disorder in the wire.

Since the zero-voltage conductance $G(\mu, 0)$ satisfies

$$\langle G(\mu, 0)\rangle = G_0 N/[1 + x(\mu)] \tag{9}$$

we may eliminate N and write equation (7) in the alternative form

$$[\langle g(\mu, W)\rangle - \langle G(\mu, W)\rangle]/\langle G(\mu, 0)\rangle = 3sW^2\, x/(1+x)^{1+\nu}. \tag{10}$$

Equations (7) and (10) hold for configurationally averaged quantities. These equations do not apply to individual wires.

3. Numerical calculations

We now consider a model numerical example to see whether equation (7) is obeyed. The method for the calculation has been presented in detail elsewhere [39]. We consider two semi-infinite perfect leads connected by a wire. The leads and the wire have a simple square lattice structure. The width of the leads is 60 atoms and that of the wire is 10 atoms. The length of the wire is 10 atoms. The electronic structure of the system is described by a single-orbital nearest-neighbour orthonormal tight-binding model with a hopping integral of $-t < 0$. The wire contains randomly distributed impurity atoms. In the absence of an applied bias, the on-site energy is zero on the native atoms and $+6\,t$ on the impurity atoms. The Fermi level in the absence of the bias is $\mu = -1.43\,t$. There are $N = 6$ open channels in the wire at μ.

The electron eigenstates for this system may be divided into two subsets [39, 41, 42]. One subset, $\{|\Psi_1\rangle\}$ with energies $\{E_1\}$, consist of a right-travelling Bloch wave incident upon the wire from the left electrode, partially reflected back into the left electrode and partially transmitted though the wire into the right electrode, and conversely for the other subset, $\{|\Psi_2\rangle\}$ with energies $\{E_2\}$. A battery of voltage W, connected across the leads, populates the states $\{|\Psi_1\rangle\}$ with a Fermi–Dirac occupation function f_1 with electrochemical potential $\mu_1 = \mu + eW/2$, and it populates the states $\{|\Psi_2\rangle\}$ with a Fermi–Dirac occupation function f_2 with electrochemical potential $\mu_2 = \mu - eW/2$. The electrons in the current-carrying lead–wire–lead system are described by the one-electron density matrix [39]

$$\rho = \int f_1(E) D_1(E)\, \mathrm{d}E + \int f_2(E) D_2(E)\, \mathrm{d}E \tag{11}$$

where

$$D_1(E) = \sum_1 |\Psi_1\rangle \delta(E - E_1) \langle\Psi_1| \qquad D_2(E) = \sum_2 |\Psi_2\rangle \delta(E - E_2) \langle\Psi_2|.$$

The total current in the system is given by $I = \mathrm{Tr}[\mathcal{I}\rho]$, where

$$\mathcal{I} = (e/\mathrm{i}\hbar)(P_2 H P_1 - P_1 H P_2)$$

is the tight-binding current operator [39,41,42]. Here H is the tight-binding Hamiltonian, and

$$P_1 = \sum_1 |1\rangle\langle 1| \qquad P_2 = \sum_2 |2\rangle\langle 2|$$

where $\{|1\rangle\}$ and $\{|2\rangle\}$ are the tight-binding positional basis states on atoms lying to the left and to the right, respectively, of an arbitrary open surface through the system. In the limit of zero temperature, assumed throughout the paper, we obtain

$$I = \int_{\mu_2}^{\mu_1} \mathrm{Tr}[\mathcal{I} D_1(E)]\, \mathrm{d}E. \tag{12}$$

The zero-voltage conductance at Fermi energy μ is given by [39]

$$G(\mu, 0) = 2e\, \mathrm{Tr}[\mathcal{I} D_1(\mu)] \tag{13}$$

where D_1 is evaluated in the absence of the applied bias, and we have included a factor of 2 for spin degeneracy. It has been shown [39] that equation (13) is equivalent to earlier expressions [41, 42] for $G(\mu, 0)$.

Within a Thomas–Fermi-type approximation, to lowest order in the battery voltage W, the on-site energy on atom n in the presence of the bias is shifted relative to its value in the absence of the bias by an amount of eW_n, where [39]

$$W_n = W(D_{1_{nn}}/D_{nn} - 1/2). \tag{14}$$

Here, $D_{1_{nn}}$ and D_{nn} are the on-site matrix elements on atom n of the operators $D_1(\mu)$ and $D(\mu) = D_1(\mu) + D_2(\mu)$, respectively, evaluated in the absence of the bias. The bias-induced on-site potential shifts $\{W_n\}$ represent the additional self-consistent potential in the system in the presence of the applied bias, whose gradient gives the local transport field, driving the current [39]. At finite bias, $D_1(E)$, and hence I in equation (12), is calculated in the presence of these on-site energy shifts.

We now consider a wire containing two impurities. Figure 1 shows a plot of $\{W_n\}$, in units of the battery voltage W. The impurity atoms in the wire are indicated by the broken arrows. The potential deep inside each lead flattens out. There is an overall potential drop from left to right. The lighter region immediately in front of each impurity and the darker region immediately behind it show the formation of a resistivity dipole across the impurity. These

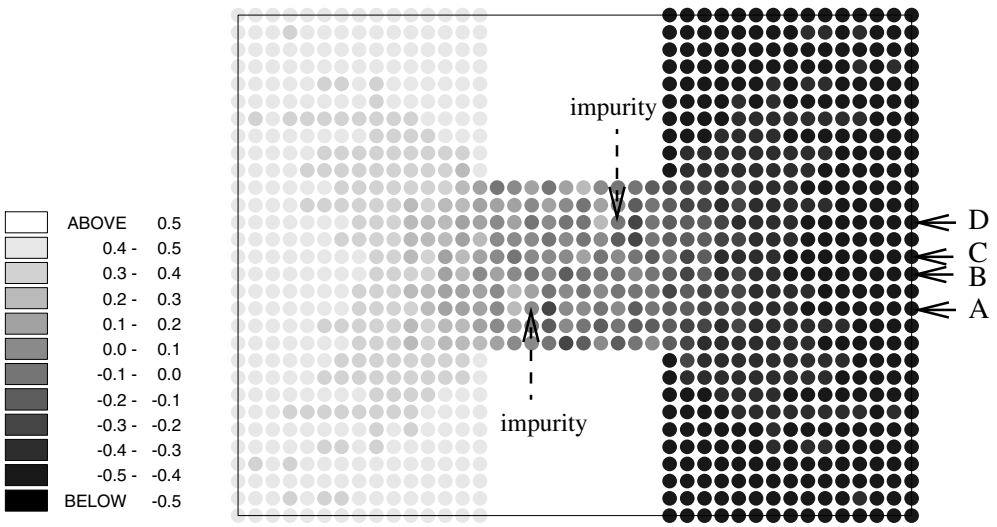

Figure 1. The bias-induced on-site potential shifts in the lead–wire–lead system in units of the battery voltage W. The wire contains two impurities, indicated by the broken arrows. Only a section of the full 60-atom cross-section of the leads is shown in the plot.

features can be seen clearly by plotting the potential along atom rows A, B, C and D from figure 1. These plots are shown in figure 2. The points corresponding to the two impurities, in the bottom and top plot in figure 2, respectively, are circled. The resistivity dipole across each impurity appears as a potential hump in front of the impurity and a potential trough behind it, superimposed on the overall background potential drop. The potential shows also some interference oscillations.

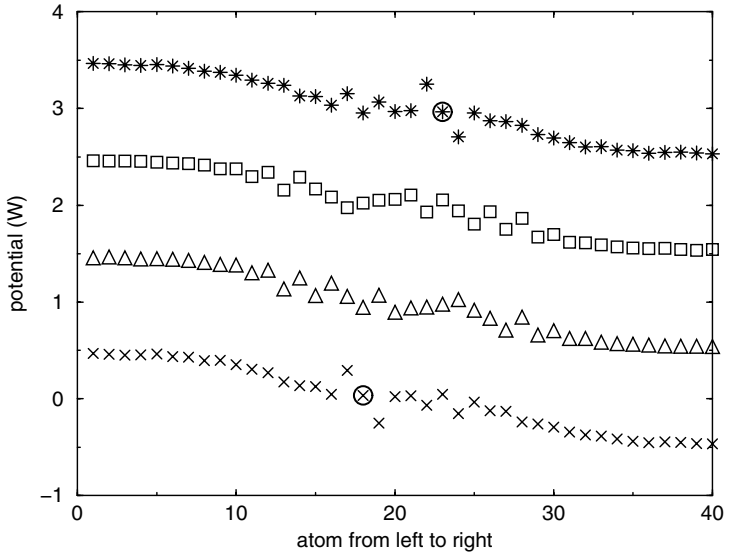

Figure 2. The bias-induced on-site potential shifts, in units of W, from left to right, along atom rows A (crosses), B (triangles), C (squares) and D (stars) of the lead–wire–lead system from figure 1. The plots for rows B, C and D are shifted vertically by one, two and three units, respectively, for clarity. The first fifteen atoms in each row lie in the left lead and the last fifteen lie in the right lead. The points corresponding to the two impurities, in the bottom and top plot, respectively, are circled.

If the leads had infinite transverse size, then the potential would reach up to $+W/2$ deep inside the left lead and down to $-W/2$ deep inside the right lead [33,39,43,44]. In the present example, where the cross-section of the leads is much greater, but not infinitely greater, than that of the connecting wire, the potential falls just short of these limiting values. In the actual calculation of the current under finite voltage, the on-site potentials are set equal to the values given by equation (14) within all wire atoms and within the first seven layers of each lead. The potential is set to $+W/2$ over the rest of the left lead and $-W/2$ over the rest of the right lead. The calculation of the operators D_1 and D, needed to evaluate equations (12), (13) and (14), uses a standard Green-function method and has been described elsewhere [39,41]. The integration in equation (12) uses an energy step of $\Delta E = 0.004\,t$. The differential conductance is obtained by taking the difference between currents for successive voltages and dividing it by the voltage increment $\Delta E/e$.

Figure 3 shows the zero-voltage conductance as a function of Fermi energy for the lead–wire–lead system with the two impurities (solid line). The zero-voltage conductance for the case without the impurities is also shown for comparison (broken line). The conductance for the impurity-free system shows a typical ballistic conductance staircase in steps of $G_0 = 2e^2/h$. The oscillations on each plateau are due to multiple reflections from the ends of the wire [45]. The introduction of the two impurities suppresses the zero-voltage conductance.

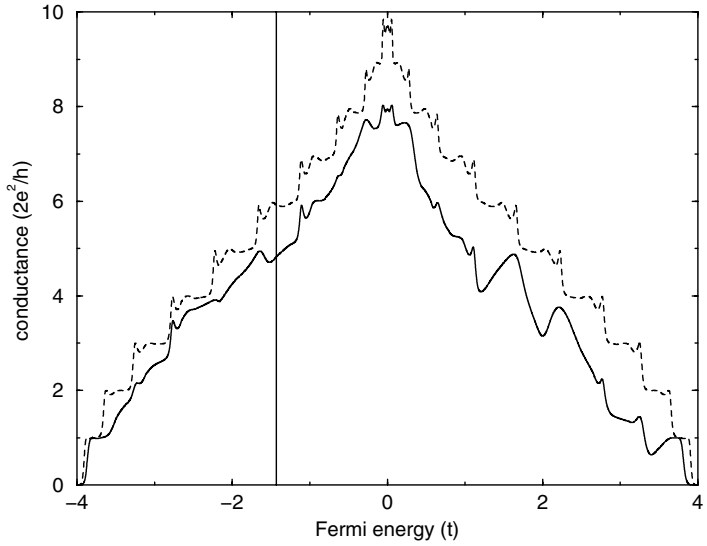

Figure 3. The zero-voltage conductance, in units of $2e^2/h$, versus Fermi energy, in units of the nearest-neighbour hopping integral t, for the system from figure 1 (solid line). The conductance for the case where there are no impurities in the wire is also shown for comparison (broken line). The vertical line at energy $-1.43\,t$ shows the position of the Fermi level μ used for the rest of the calculations.

Figure 4 shows the differential conductance $G(\mu, W)$ (solid line) and the quantity $g(\mu, W)$ from equation (8) (broken line) versus battery voltage W, for the system with the two impurities. The plot illustrates the behaviour, given by equation (7). G follows g in overall shape but

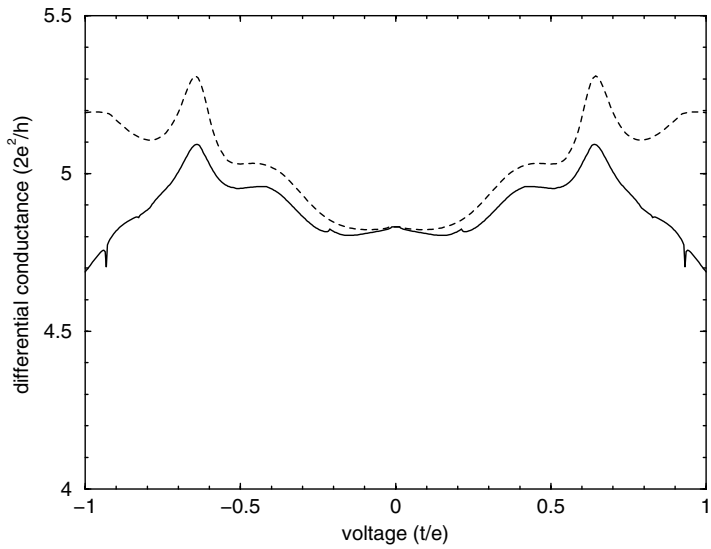

Figure 4. The differential conductance $G(\mu, W)$ (solid line) and the quantity $g(\mu, W) = [G(\mu + eW/2, 0) + G(\mu - eW/2, 0)]/2$ (broken line) versus battery voltage for the lead–wire–lead system with the two impurities.

is suppressed below g in magnitude. An interesting feature of the plot is the cusps in the differential conductance. These cusps, not all of which are resolved with the present energy step ΔE, correspond to the opening or closing of conductance channels in the leads. Test calculations on smaller systems showed that in general, in the presence of disorder in the wire, the existence of a subband edge at energy $\mu + eW$ in the perfect lead in the unbiased system results in cusps in the quantities $G(\mu+eW, 0)$, $G(\mu, \pm W)$ and $g(\mu, 2W)$. Here, this effect will not be investigated further, except to note that past calculations have reported sharp, cusp-like variations in the zero-voltage conductance near subband edges in disordered wires [45, 46].

Equation (7) is now tested in the following way. The wire is given a random distribution of impurities with a fractional concentration p. For each value of p, $G(\mu, W)$ and $g(\mu, W)$ are calculated for voltages from $W = -0.12\,t/e$ to $W = +0.12\,t/e$ and are averaged over 50 impurity configurations. The value of $x = L/l_0$ for that p is inferred from equation (9). A quadratic in W is fitted to $(\langle g\rangle - \langle G\rangle)/G_0$ and the coefficient of W^2, c_W, is plotted as a function of x. This plot is shown in figure 5 (crosses). The ten points from left to right correspond to $p = 0.01\,m$ with $m = 1, \ldots, 10$, respectively. According to equation (7), $c_w = 3Ns\,x/(1+x)^{2+\nu}$. Also shown in figure 5 is a plot of this function with $s = 0.5\,e^2/t^2$ and $\nu = 1$ (solid line).

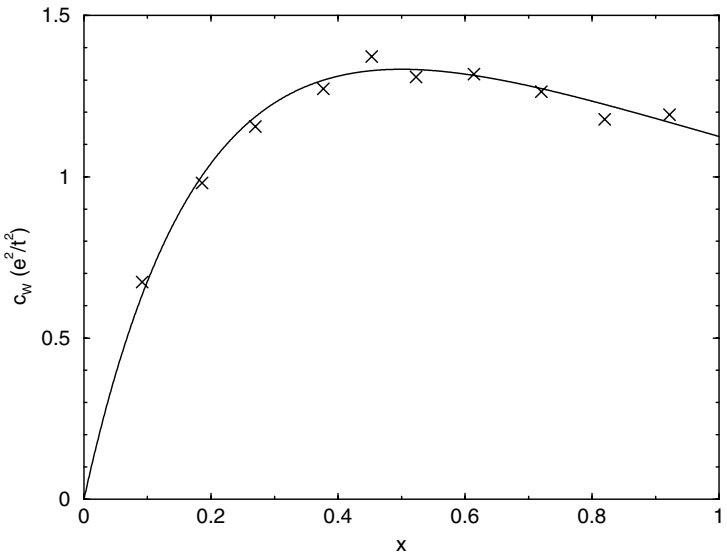

Figure 5. The coefficient, c_W, of W^2 in $[\langle g(\mu, W)\rangle - \langle G(\mu, W)\rangle]/G_0$ versus $x = L/l_0$ (crosses). The curve $c_w = 3Ns\,x/(1+x)^{2+\nu}$ with $N = 6$, $s = 0.5$ and $\nu = 1$ is also shown for comparison (solid line).

4. Discussion and summary

The results in figure 5 support equation (7). To within an order of magnitude, the value for s of $0.5\,e^2/t^2$, obtained from the fit, may be understood as follows. Place a lone impurity in a ballistic wire. Apply a voltage W. A resistivity dipole forms around the impurity. Let the lobe of the resistivity-dipole potential in front of the impurity reach up to $+\xi W/2$, and let that behind the impurity reach down to $-\xi W/2$. Let each lobe of the dipole potential extend laterally over ζ atoms, where ξ and ζ are numbers of order unity. Embed this dipole

potential in an infinite perfect simple square lattice. Then, treating the two lobes as independent scatterers with additive cross-sections and using the Fermi golden rule, we may estimate the scattering cross-section of the dipole as $\sigma_W = \pi\eta e^2 W^2 \rho_\mu a^2/(\hbar v_\mu)$, where $\eta = \xi^2\zeta$, ρ_μ is the Fermi density of states per atom, a is the lattice parameter, and v_μ is the average of the Fermi velocity over the Fermi surface for the infinite square lattice. Note that, as is appropriate in two dimensions, the cross-section has units of length. The Green function, and hence the density of states, for the infinite square lattice can be evaluated by Brillouin zone integration, giving $\rho_\mu = 0.125\,t^{-1}$. As an estimate of v_μ, take the Fermi velocity in the [11] direction, given by $2\sqrt{2}at\sin[\cos^{-1}(-\mu/4t)]/\hbar$. This gives $\sigma_W = 0.15\eta\, e^2 W^2 a/t^2$. Assuming that the cross-section of the impurity, σ_d, is comparable to a, for $s = \sigma_W/(W^2\sigma_d)$ we find a value of $0.15\eta\, e^2/t^2$, compatible with that obtained from the fit in figure 5.

Let us now discuss the limitations of the model in the paper. To derive equation (6), we ignored electron backscattering by the smooth average background potential, on which the dipole potentials are superimposed. This background potential will in general cause some reflection, which will lead to an additional suppression of the transmission through the wire, as seen for example in recent calculations on defect-free ballistic atomic chains [47]. Let us estimate the size of the effect. Let the background potential drop of W be realized over a length of the order of $L = N_L a$, where N_L is the number of atoms along the wire. In reality the background potential drop extends over parts of the leads too, making the length in question larger than the wire length, but we will ignore this here for simplicity. Think of this background potential as a series of N_L potential steps of height W/N_L. Treating each step as a weak scatterer, a free-electron calculation in one dimension gives for the total reflection probability of the N_L steps $R_L = (eW/E_F)^2/(16N_L)$, where E_F is the Fermi energy in the free-electron model. From equation (6), on the other hand, we may identify the total reflection probability due to the distribution of resistivity-dipole potentials as $R_W = sxW^2/(1+x)^\nu$. Then, with $s = 0.5\,e^2/t^2$ and with t and E_F of the order of eV, R_W/R_L will be of the order of $8N_L x/(1+x)^\nu$. For any value of x, therefore, we can always make R_W dominate R_L by making N_L large enough. In particular, with allowances for the crudeness of the argument, for intermediate values of x around unity, R_W will dominate R_L for $N_L > 10$.

Another limitation of the earlier analysis is the assumed empirical relation between σ_W and $x = L/l_0$ in equation (5). That equation was introduced as a trial form for intermediate values of x. As indicated earlier, the true dependence of σ_W on x ought to reduce to $\sigma_W^0 W^2/x^2$ in the extreme diffusive limit.

The most serious approximation in the paper is in the treatment of the scattering by the dipole potentials. We have treated the resistivity dipoles and the intrinsic defects as independent scattering mechanisms that add in series. In the limit where each defect can be treated as a weak scatterer, this assumption can be justified as follows. Consider a lone substitutional impurity with on-site energy v_d, placed at the origin in an otherwise perfect infinite crystal. Illuminate the impurity by a uniform current density. Let $V = V_d + V_W$ be the self-consistent tight-binding potential in the presence of the current, where $V_d = |0\rangle v_d \langle 0|$ is the scattering potential of the impurity, and $V_W = \sum_n |n\rangle W_{\boldsymbol{R}_n} \langle n|$ is the additional self-consistent potential in the presence of the current. Here $|n\rangle$ is the tight-binding basis state at atom n with position $\boldsymbol{R}_n$, with the impurity atom labelled as 0. The on-site energy shifts $\{W_{\boldsymbol{R}_n}\}$ constitute the resistivity-dipole potential. To lowest order in the current, $W_{\boldsymbol{R}_n}$ is linear in the current. This, together with the inversion symmetry of the system, implies that $W_{\boldsymbol{R}_n}$ is an odd function of $\boldsymbol{R}_n$, $W_{\boldsymbol{R}_n} = -W_{-\boldsymbol{R}_n}$. Consider now the matrix element $\langle \boldsymbol{k}|V|\boldsymbol{k}'\rangle$ for scattering between two Bloch-wave states

$$|\boldsymbol{k}\rangle = \sum_n \exp(\mathrm{i}\boldsymbol{R}_n \cdot \boldsymbol{k})|n\rangle \qquad |\boldsymbol{k}'\rangle = \sum_n \exp(\mathrm{i}\boldsymbol{R}_n \cdot \boldsymbol{k}')|n\rangle.$$

Using the property $W_{\boldsymbol{R}_n} = -W_{-\boldsymbol{R}_n}$, it is easy to show that

$$|\langle \boldsymbol{k}|V|\boldsymbol{k}'\rangle|^2 = |\langle \boldsymbol{k}|V_d|\boldsymbol{k}'\rangle|^2 + |\langle \boldsymbol{k}|V_W|\boldsymbol{k}'\rangle|^2.$$

Therefore, within the Fermi golden rule, $\sigma = \sigma_d + \sigma_W$, where σ is the scattering cross-section of the combined potential V, and σ_d and σ_W are the separate cross-sections of the impurity potential V_d and the dipole potential V_W, respectively. Equation (3) follows. However, in the case of strong impurity scattering, the cross-section of the combined potential may contain significant higher-order mixed terms in V_d and V_W. These higher-order interference corrections are ignored in equation (3).

In our estimate of the dipole cross-section and the quantity s above, we have ignored the long-range behaviour of the dipole and have treated the dipole as a simple localized scatterer. In reality, while the dipole potential does have localized lobes in the immediate vicinity of the defect, it also has complex long-ranged tails [37, 38]. This will affect the value of σ_W and will introduce some environment dependence in σ_W and in s.

A more rigorous calculation should treat the defect and its associated resistivity-dipole potential as a single entity and should allow for the long-range behaviour of the dipole. A particular line of thought to be explored by more detailed calculations is this. It is tempting to imagine that the lateral spatial extent of the lobes of the resistivity-dipole potential will be roughly proportional to the lateral extent of the defect that gives rise to the dipole. The scattering cross-section of the dipole would then be roughly proportional to that of the defect, making the quantity $s \propto \sigma_W/\sigma_d$ in equations (7) and (10) relatively insensitive to the precise nature of the defect. That would make s an intrinsic property of the metal, determined by its electronic properties at the Fermi level. Equations (7) and (10) would hold whatever the defects in the wire, and, if scattering rates due to different defects are additive, these equations would hold also when more then one type of defect is present. The validity, or otherwise, of this guess depends crucially on the long-range details of the dipole potential.

Experimental measurements of the finite-voltage differential conductance of atomic-scale metallic contacts are available. Some measurements show a pronounced quadratic increase in conductance with voltage [22, 48], while others show no evidence for such an increase [49, 50]. It has been suggested recently [51] that the large non-linearities in the current–voltage characteristics are due to tunnelling through a contaminant layer between the electrodes, whereas for clean point contacts, the current–voltage relation is almost linear. Tunnelling effects are not included in equations (7) and (10) and in an experimental test of these equations it would therefore be necessary to ensure that such effects are not present.

A difficulty in testing equations (7) and (10) experimentally is the appearance in them of the quantity $g = [G(\mu + eW/2, 0) + G(\mu - eW/2, 0)]/2$. To measure g directly, it would be necessary to probe the zero-voltage conductance away from the Fermi level. Else, it would be necessary to make an assumption about g. For instance, one could assume that, at least for modest amounts of strong, semi-classical scatterers, the electron mean free path l_0, and hence the configurationally averaged zero-voltage conductance, is independent of energy, in which case $\langle g\rangle$ may be treated as independent of W.

In conclusion, the self-consistent effective potential in a current-carrying disordered quantum wire is non-uniform due to the formation of resistivity dipoles across scattering centres. It is argued here that these non-uniformities in the potential result in a suppression of the conductance of such a wire at finite voltage. The suppression is related directly to the intrinsic scattering in the wire via equations (7) and (10). These equations have been derived by an unrigorous, semi-classical argument and they may be viewed only as model semi-empirical relations. Nonetheless, they are borne out by numerical calculations, and they express a general point: the suppression of the differential conductance at finite voltage is a

function of the quantity $x = L/l_0$, and this suppression vanishes in the ballistic and diffusive limits, peaking in between, for values of x comparable to unity. Conductance fluctuations are related to the elastic electron mean free path l_0 in a nanojunction [29]. That, combined with determination of the quantity $x = L/l_0$ along the lines outlined above, could allow the actual effective length L of a nanojunction to be inferred solely from its differential conductance.

Acknowledgments

This paper grew out of discussions with Jan van Ruitenbeek, Kim Hansen, John Hoekstra and Adrian Sutton. The author is grateful to the referees for helpful comments. The author thanks the Engineering and Physical Sciences Research Council for support through an Advanced Fellowship.

References

[1] van Wees B J, van Houten H, Beenakker C W J, Williamson J G, Kouwenhoven L P, van der Marel D and Foxon C T 1988 *Phys. Rev. Lett.* **60** 848
[2] Wharam D A, Thornton T J, Newbury R, Pepper M, Ahmed H, Frost J E F, Hasko D G, Peacock D C, Ritchie D A and Jones G A C 1988 *J. Phys. C: Solid State Phys.* **21** L209
[3] Muller C J, van Ruitenbeek J M and de Jongh L J 1992 *Phys. Rev. Lett.* **69** 140
[4] Krans J M, Muller C J, Yanson I K, Govaert Th C M, Hesper R and van Ruitenbeek J M 1993 *Phys. Rev.* B **48** 14 721
[5] Agrait N, Rodrigo J G and Vieira S 1993 *Phys. Rev.* B **47** 12 345
[6] Agrait N, Rodrigo J G, Sirvent C and Vieira S 1993 *Phys. Rev.* B **48** 8499
[7] Pascual J I, Mendez J, Gomez-Herrero J, Baro A M, Garcia N and Binh V T 1993 *Phys. Rev. Lett.* **71** 1852
[8] Todorov T N and Sutton A P 1993 *Phys. Rev. Lett.* **70** 2138
[9] Landman U, Luedtke W D, Salisbury B E and Whetten R L 1996 *Phys. Rev. Lett.* **77** 1362
[10] Todorov T N and Sutton A P 1996 *Phys. Rev.* B **54** 14 234
[11] Sorensen M R, Brandbyge M and Jacobsen K W 1998 *Phys. Rev.* B **57** 3283
[12] Agrait N, Rubio G and Vieira S 1995 *Phys. Rev. Lett.* **74** 3995
[13] Rubio G, Agrait N and Vieira S 1996 *Phys. Rev. Lett.* **76** 2302
[14] Stalder A and Dürig U 1996 *Appl. Phys. Lett.* **68** 637
[15] Torres J A, Pascual J I and Saenz J J 1994 *Phys. Rev.* B **49** 16 581
[16] Bogachek E N, Scherbakov A G and Landman U 1997 *Phys. Rev.* B **56** 1065
[17] Bratkovsky A M, Sutton A P and Todorov T N 1995 *Phys. Rev.* B **52** 5036
[18] Brandbyge M, Jacobsen K W and Norskov J K 1997 *Phys. Rev.* B **55** 2637
[19] Olesen L, Laegsgaard E, Stensgaard I, Besenbacher F, Schiotz J, Stoltze P, Jacobsen K W and Norskov J K 1994 *Phys. Rev. Lett.* **72** 2251
[20] Krans J M, van Ruitenbeek J M, Fisun V V, Yanson I K and de Jongh L J 1995 *Nature* **375** 767
[21] Muller C J, Krans J M, Todorov T N and Reed M A 1996 *Phys. Rev.* B **53** 1022
[22] Costa-Krämer J L, Garcia N, Garcia-Mochales P, Serena P A, Marques M I and Correia A 1997 *Phys. Rev.* B **55** 5416
[23] Kouwenhoven L P, van Wees B J, Harmans C J P M, Williamson J G, van Houten H, Beenakker C W J, Foxon C T and Harris J J 1989 *Phys. Rev.* B **39** 8040
[24] Glazman L I and Khaetskii A V 1989 *Europhys. Lett.* **9** 263
[25] Castano E and Kirczenow G 1990 *Phys. Rev.* B **41** 3874
[26] Martin-Moreno L, Nicholls J T, Patel N K and Pepper M 1992 *J. Phys.: Condens. Matter* **4** 1323
[27] Xu H 1993 *Phys. Rev.* B **47** 15 630
[28] Pascual J I, Torres J A and Saenz J J 1997 *Phys. Rev.* B **55** 16 029
[29] Ludolph B, Devoret M H, Esteve D, Urbina C and van Ruitenbeek J M 1999 *Phys. Rev. Lett.* **82** 1530
[30] Sivan U and Imry Y 1986 *Phys. Rev.* B **33** 551
[31] Landauer R 1987 *Z. Phys.* B **68** 217
[32] Pernas P L, Martin-Rodero A and Flores F 1990 *Phys. Rev.* B **41** 8553
[33] McLennan M J, Lee Y and Datta S 1991 *Phys. Rev.* B **43** 13 846
[34] Ulreich S and Zwerger W 1998 *Superlatt. Microstruct.* **23** 719

[35] Landauer R 1957 *IBM J. Res. Dev.* **1** 223
[36] Landauer R 1988 *IBM J. Res. Dev.* **32** 306
[37] Payne M C and Engel G E 1990 *J. Phys.: Condens. Matter* **2** 1355
[38] Sorbello R S 1981 *Phys. Rev.* B **23** 5119
[39] Todorov T N 1999 *Phil. Mag.* B **79** 1577
[40] Büttiker M, Imry Y, Landauer R and Pinhas S 1985 *Phys. Rev.* B **31** 6207
[41] Todorov T N 1996 *Phys. Rev.* B **54** 5801
[42] Todorov T N, Briggs G A D and Sutton A P 1993 *J. Phys.: Condens. Matter* **5** 2389
[43] Landauer R 1989 *J. Phys.: Condens. Matter* **1** 8099
[44] Landauer R 1992 *Phys. Scr.* T **42** 110
[45] Todorov T N and Briggs G A D 1994 *J. Phys.: Condens. Matter* **6** 2559
[46] Garcia-Mochales P, Serena P A, Garcia N and Costa-Krämer J L 1996 *Phys. Rev.* B **53** 10 268
[47] Brandbyge M, Kobayashi N and Tsukada M 1999 *Phys. Rev.* B **60** 17 064
[48] Abellan J, Chocon R and Arenas A 1988 *Surf. Sci.* **418** 493
[49] Yasuda H and Sakai A 1997 *Phys. Rev.* B **56** 1069
[50] Itakura K, Yuki K, Kurokawa S, Yasuda H and Sakai A 1999 *Phys. Rev.* B **60** 11 163
[51] Hansen K, Nielsen S K, Brandbyge M, Laegsgaard E, Stensgaard I and Besenbacher F 2000 *Appl. Phys. Lett.* **77** 708